Philosophical Magazine

ISSN: 1478-6435 (Print) 1478-6443 (Online) Journal homepage: http://www.tandfonline.com/loi/tphm20

Structure factor determination of deuterated 1- and 2-propanol using diffraction experiments with polarization analysis

L.A. Rodríguez Palomino, G.J. Cuello, A. Stunault & J. Dawidowski

To cite this article: L.A. Rodríguez Palomino, G.J. Cuello, A. Stunault & J. Dawidowski (2015): Structure factor determination of deuterated 1- and 2-propanol using diffraction experiments with polarization analysis, Philosophical Magazine, DOI: 10.1080/14786435.2015.1102350

To link to this article: http://dx.doi.org/10.1080/14786435.2015.1102350

Philosophical Magazine, 2015
http://dx.doi.org/10.1080/14786435.2015.1102350

Taylor & Francis
Taylor & Francis Group

Structure factor determination of deuterated 1- and 2-propanol using diffraction experiments with polarization analysis

L.A. Rodríguez Palomino[ab*], G.J. Cuello[a], A. Stunault[a] and J. Dawidowski[b]

[a]*Institut Laue Langevin, 71, av des Martyrs, 38042 Grenoble, France;* [b]*Consejo Nacional de Investigaciones Científicas y Técnicas, Centro Atómico Bariloche and Instituto Balseiro, Bustillo 9500 (R8402AGP), Bariloche, Argentina*

(*Received 6 July 2015; accepted 25 September 2015*)

We present the experimental structure factors of deuterated 1- and 2-propanol as determined at the Spin Polarized Hot Neutron Beam Facility (D3) of the Institut Laue Langevin. Polarized neutron scattering with polarization analysis has the advantage of experimentally separating the coherent and incoherent scattering intensities. Using a linear combination of non-spin-flip and spin-flip diffractograms, one can determine the coherent intensity, related to the structure factor. The corrections of experimental data for multiple scattering, attenuation and inelasticity are carried out using a Monte Carlo (MC) simulation code developed for this kind of experiments. This (hybrid) MC method is based on the combination of a modelled energy exchange and the experimental angular distribution. The good agreement observed between our simulations and the experimental results, confirms the goodness of this model. We also compare our results with experimental data from other authors and we stress the need of more experimental data in the low-Q region.

Keywords: liquids; Monte Carlo; neutron diffraction; polarization; structure

1. Introduction

In hydrogen-containing molecules, hydrogen often plays a key role, since many properties are derived directly from the inter-molecular hydrogen bond. For such molecules, neutron scattering, with high scattering contrast is ideally suited to study the structural and dynamical properties. However, due to the additional complexity of the enormous incoherent signal from hydrogen, most studies have, up to now, been performed on deuterated samples.

Using polarized neutron diffraction with polarization analysis, one can almost directly measure the incoherent cross section [1]: since the neutron has a spin 1/2, it is sensitive to the nuclear spin, giving different scattering intensities, whether the nuclear spins are parallel or anti-parallel to the neutron polarization. This is the source of the (spin) incoherent scattering observed for hydrogen, but also the basis of the method proposed here. Experimentally, using a set of polarizers/analysers, one can measure separately the scattered intensities with polarization parallel (non-spin-flip, NSF) or anti-parallel (spin-flip, SF) to the primary beam polarization (see Section 2 for details). Simple linear relationships then lead from

*Corresponding author. Email: rodrigl@cab.cnea.gov.ar

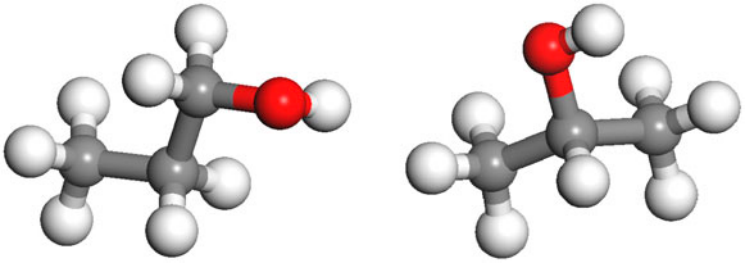

1-propanol **2-propanol**

Figure 1. (colour online) Molecular structure of the 1- and 2-propanol, $CD_3CD_2CD_2OD$ and $CD_3CD(OD)CD_3$, respectively. Red (dark grey in b/w version), light grey and grey spheres are O, D and C, respectively.

the measured NSF/SF intensities to the incoherent and coherent scattering cross sections (Section 5).

The traditional [2–4] or new empirical [1] methods for correcting for background, attenuation, inelasticity and multiple scattering treat all these contributions independently and not as a whole. In Sections 3 and 4, we propose a consistent treatment of all corrections, based on a Monte Carlo (MC) simulation of the neutron–sample interaction (Section 4). Compared to traditional [2–4] or new empirical [1] methods, this one should represent a step forward, towards more accurate data corrections.

In the past, the structures of the liquid phases of the lowest members in the alcohol series (methanol, ethanol and iso-propanol) have been determined by neutron diffraction [5–11], mostly from deuterated samples. As a first test, we study 1- and 2-propanol, which are rather simple molecules with a high proportion of hydrogen and ideally suited to develop and test the method. In this work, we use deuterated 1- and 2-propanol, $CD_3CD_2CD_2OD$ and $CD_3CD(OD)CD_3$ (Figure 1). The corrections are expected to be small, due to much reduced incoherent contribution, and our results can be easily compared to previous, unpolarized work (Section 5).

Finally, in Section 6, we make a careful analysis of the obtained structure factors, to gain some insight into the structures of both molecules. In particular, in the case of 2-propanol, we compare our results with those from other authors. This comparison leaves some open questions about the structure factor at low-Q, that should be resolved with new experimental evidence.

2. Experimental

The experiment was performed at the Spin Polarized Hot Neutron Beam Facility (D3) of the ILL (Institut Laue Langevin, Grenoble, France). A detailed description of the diffractometer can be found in Refs. [13,14]. The unpolarized neutron beam is monochromated and polarized using a Heusler crystal Cu_2MnAl ((1 1 1) Bragg reflection). Guide field along the beam path preserve the polarization, while nutators before and after the sample can reverse (flip) it. The neutrons scattered by the sample are analysed using a polarized ^{3}He spin filter [15,16] and the transmitted neutrons are collected in a single ^{3}He detector scanned over an

angular range $2\theta = 4° - 120°$. With a wavelength of 0.52 Å, the NSF and SF diffractograms are recorded for a momentum transfer of 0.8–21 Å^{-1} ($Q = \frac{4\pi}{\lambda} \sin\theta$).

The samples of fully deuterated 1-propanol (98%at. D) and 2-propanol (99%at. D) were bought from Isotec Inc. and Aldrich Chemical Co, respectively, and the experiments were performed in the liquid state at room temperature. The macroscopic densities (ρ) and isothermal compressibilities (χ_T) are: 0.912 g/cm^3 (or 0.00806 at./Å^3) [17] and 1.21×10^{-9} Pa^{-1} [11] for deuterated 1-propanol, and 0.890 g/cm^3 (or 0.00787 at./Å^3) [17] and 1.12×10^{-9} Pa^{-1} [11] for deuterated 2-propanol. The densities will be used in the normalization process to obtain the structure factor on an absolute scale. The samples were loaded into a cylindrical double-walled vanadium cell (hollow cylinder) of 10.7 mm external diameter, 7.7 mm internal diameter, 0.15 mm walls thickness and 58 mm height, giving a sample thickness of 1.2 mm and a volume of 0.829 cm^3 in the beam. The mass was checked before and after the experiment, confirming that the container had no leakage.

Measurements of NSF and SF diffractograms were carried out for a period of 24 h for each sample. The signal from the empty instrument, the empty vanadium container and a vanadium rod (10 mm diameter by 60 mm height) were measured in shorter times. Short measurements were periodically performed on a Ge single crystal placed at the sample position [14] to monitor the analysing power of the ^{3}He spin filter. All diffractograms were corrected for the absorption by the empty ^{3}He filter and normalized to the monitor counts. Figure 2 shows the NSF/SF diffractograms for 1-propanol after correcting for the spin-filter efficiency: empty instrument background $I^{\mathrm{B}}_{\mathrm{exp}}(Q)^{\mathrm{NSF,SF}}$, sample container (+background) $I^{\mathrm{CB}}_{\mathrm{exp}}(Q)^{\mathrm{NSF,SF}}$ and sample (+container+background) $I^{\mathrm{SCB}}_{\mathrm{exp}}(Q)^{\mathrm{NSF,SF}}$. In the low-$Q$ range, the background subtraction is a delicate issue because the empty instrument signal becomes comparable to those of the sample and the container.

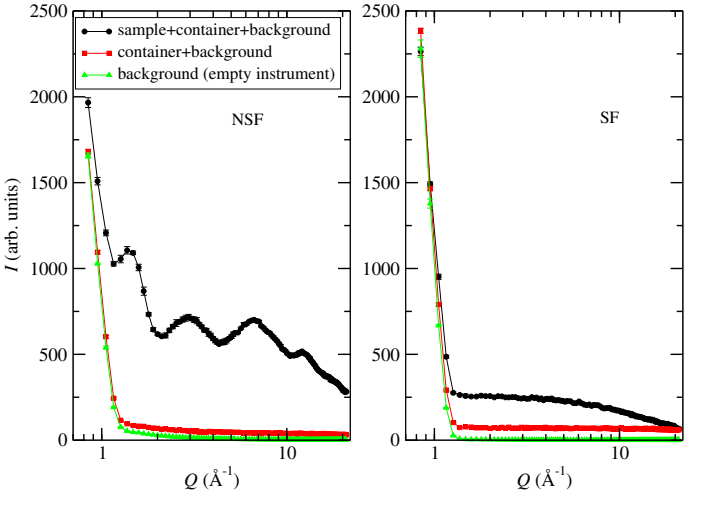

Figure 2. (colour online) Experimental diffractograms (NSF/SF) for deuterated 1-propanol, empty container and background. The logarithmic scale in the abscissa emphasizes the low-Q region.

3. Data treatment

Starting with the measured NFS/SF diffractograms described in the previous section, we first determine the experimental NSF/SF intensities scattered by the sample alone, $I^{\mathrm{S}}(Q)^{\mathrm{NSF,SF}}$. In contrast with traditional methods, we use a new procedure that results in a more precise determination of this magnitude, as explained below.

The first step, background subtraction, must be handled with special care. It cannot be done simply subtracting the empty instrument signal, because the actual background is affected by attenuation in the scatterer at the sample position. Thus, the background to be subtracted from the sample+container measurement is the empty instrument signal multiplied by the attenuation coefficient of the sample+container ($\mathrm{A}^{\mathrm{SC}}(Q)$). For the empty container measurement, we proceed the same way using the empty container attenuation coefficient $\mathrm{A}^{\mathrm{C}}(Q)$. The analytical expressions for both coefficients have been defined by Sears as the *primary attenuation coefficients* [18]. We must stress that an improper background subtraction produces an anomalous behavior of the structure factor at low-Q, where the empty instrument signal is highest.

Once we have determined the sample+container and container background-corrected diffractograms, we must subtract the container contribution from the sample+container signal. For that, we need to calculate another attenuation factor defined as the ratio between the intensity scattered by the container and attenuated by the sample+container $\mathrm{I}^{\mathrm{C,SC}}(Q)^{\mathrm{NSF,SF}}$ and the intensity scattered by the container and attenuated by the container $\mathrm{I}^{\mathrm{C,C}}(Q)^{\mathrm{NSF,SF}}$.

We have calculated these attenuation coefficients and scattering factors using a MC simulation code, which will be described in Section 4. The experimental intensity $I^{\mathrm{S}}(Q)^{\mathrm{NSF,SF}}$ is then

$$I^{\mathrm{S}}(Q)^{\mathrm{NSF,SF}} = \overbrace{\left[I^{\mathrm{SCB}}_{\mathrm{exp}}(Q)^{\mathrm{NSF,SF}} - A^{\mathrm{SC}}(Q)\; I^{\mathrm{B}}_{\mathrm{exp}}(Q)^{\mathrm{NSF,SF}}\right]}^{\text{background correction to sample+container}} - \underbrace{\frac{\mathrm{I}^{\mathrm{C,SC}}(Q)^{\mathrm{NSF,SF}}}{\mathrm{I}^{\mathrm{C,C}}(Q)^{\mathrm{NSF,SF}}}}_{\text{attenuation factor}} \underbrace{\left[I^{\mathrm{CB}}_{\mathrm{exp}}(Q)^{\mathrm{NSF,SF}} - A^{\mathrm{C}}(Q)\; I^{\mathrm{B}}_{\mathrm{exp}}(Q)^{\mathrm{NSF,SF}}\right]}_{\text{background correction to container}} . \quad (1)$$

It is worth mentioning that Equation (1) represents the total number of neutrons scattered by the sample alone at a given momentum transfer Q, including both single and multiple scattering. This $I^{\mathrm{S}}(Q)^{\mathrm{NSF,SF}}$ still needs to be corrected for multiple scattering and the attenuation by the sample itself. Both corrections are evaluated using our MC code: the multiple scattering factor $F_{\mathrm{mul}}(\mathbf{k_0}, Q)^{\mathrm{NSF,SF}}$ is the ratio between the single scattering and the total scattering signal as obtained from simulation, and the attenuation factor $A_{\mathrm{S,S}}(\mathbf{k_0}, Q)$ is the ratio between the attenuated single scattering and non-attenuated single scattering from the sample alone. The sample signal already corrected for all experimental effects is finally given by

$$I^{\mathrm{S}}_{\mathrm{corr}}(Q)^{\mathrm{NSF,SF}} = \frac{F_{\mathrm{mul}}(\mathbf{k_0}, Q)^{\mathrm{NSF,SF}}}{A_{\mathrm{S,S}}(\mathbf{k_0}, Q)}\; I^{\mathrm{S}}(Q)^{\mathrm{NSF,SF}} \quad (2)$$

where the pre-factor corresponds to $F(\mathbf{k_0}, Q)^{\mathrm{NSF,SF}}$, as defined by Rodríguez Palomino et al. (see [13, Equation (7)]). Figure 3 shows the intensities (NSF/SF) for deuterated 1-propanol after background and container subtraction (Equation (1)), and the insets show the

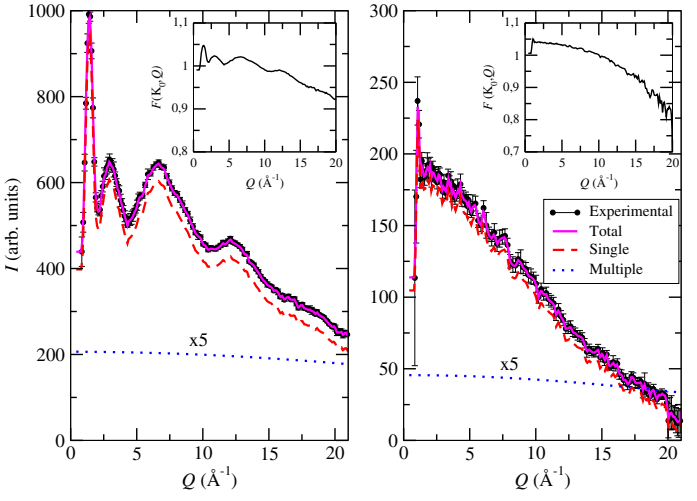

Figure 3. (colour online) Experimental NSF (left) and SF (right) intensities (symbols) compared with the MC simulation (solid line) for liquid 1-propanol. The single (dashed line) and multiple (dotted line) scattering are also shown; the latter has been multiplied by a factor 5 for the sake of visibility. The insets show the converged (NSF and SF) correction factors (pre-factor in Equation (2)).

corresponding correction factors (pre-factor in Equation (2)). Similar curves are obtained for the corresponding intensities of the deuterated 2-propanol.

4. Monte Carlo simulations

The MC simulation is based on the method proposed by Bischoff [19] and Copley et al. [20]. Using this program, one can assess the different components of the scattering distributions (single scattering, multiple scattering, attenuation factors and total scattering), which in turn will serve to determine a Q-dependent correction factor (pre-factor in Equation (2) and insets in Figure 3). This factor is then employed to correct the NSF and SF experimental intensities, and obtain the corresponding experimental single scattering intensities (see [13, Equations (1) and (2)]). In the simulation, the following magnitudes are evaluated:

(a) the incidence point on the sample surface;
(b) the scattering points in the sample or container, which are determined taking into account the corresponding path-length distribution;
(c) the neutron energy after each collision; and
(d) the neutron flight direction after each collision. Finally, the contribution of the current history to the diffractogram is scored by the detector placed at an angle 2θ with respect to the incident beam [13].

For steps (b) and (c), we need to know the total cross section as a function of the energy and the energy transfer kernels. In the case of alcohols, either there is insufficient information of both magnitudes in the literature or it is only available in a reduced energy range [21]. Since these magnitudes are essential for our simulation, we resort to their calculation using the Synthetic Model, which has been extensively discussed elsewhere [22] and successfully

Table 1. Input parameters for the Synthetic Model for 2-propanol. Columns 2–6 list the vibrational frequency ($\hbar\omega_\lambda$), their associated widths ($\hbar\sigma_\lambda$), and the D, C and O effective masses, respectively.

Mode	$\hbar\omega_\lambda$ (meV)	$\hbar\sigma_\lambda$ (meV)	M_D (amu)	M_C (amu)	M_O (amu)
CD_3 group					
1	16.3	1	27.53	23.11	–
2	31.6	2	10.93	112.0	–
3	134.4	18	5.17	252.0	–
4	300.0	18	6.2688	126.0	–
CD group					
1	16.6	1	23.249	24.146	–
2	68.0	2	67.685	117.020	–
3	113.0	18	3.944	263.295	–
4	272.0	18	6.006	131.648	–
OD group					
1	16.3	1	27.53	––	33.8
2	36.0	2	5.22	––	213.9
3	153.0	18	12.1	––	290.3
4	310.0	18	5.874	––	179.3

applied in a variety of cases [23–25]. For the angular distribution (step (d)), we employ the experimental diffractograms corrected for background and empty cell (Equation (1)). After each program run, the diffractograms are corrected and the new distributions used as new inputs, in an iterative scheme. We have thus defined an hybrid method, which relies on both the experimental angular distribution and a suitable model for the energy transfer. This scheme proved to work well for coherent samples in unpolarized neutron diffraction experiments [26].

The Synthetic Model is based on a gas model with effective masses and a set of discrete frequencies and widths with corresponding weights, defining a synthetic vibrational spectrum. This model was successfully used to describe the neutron total cross section of ethanol [25]. The propanol and ethanol molecules are very similar, sharing the same CD_3, CD_2 and OD elementary molecular units; the CD unit is present in 2-propanol alone. To construct the propanol Synthetic Model, we used the ethanol input parameters for the CD_3, CD_2 and OD units and performed a specific calculation for the CD unit of 2-propanol. In this case, we use the CD_2 vibrational modes to describe the CD modes, recalculating the effective masses of the C and D vibrational modes and keeping the same vibrational frequencies. Table 1 shows the parameters used to calculate the neutron total cross section and the energy-transfer kernels for 2-propanol.

As input, the MC program also requires the incident neutron energy, the beam dimensions, the macroscopic total cross section, the energy transfer kernel, the absorption cross section, the sample geometry, and the SF interaction probability. The latter is evaluated as the ratio between the SF cross section (2/3 of the spin-incoherent cross section) and the total scattering cross section [27]; for both propanol molecules this probability is 0.1328. The

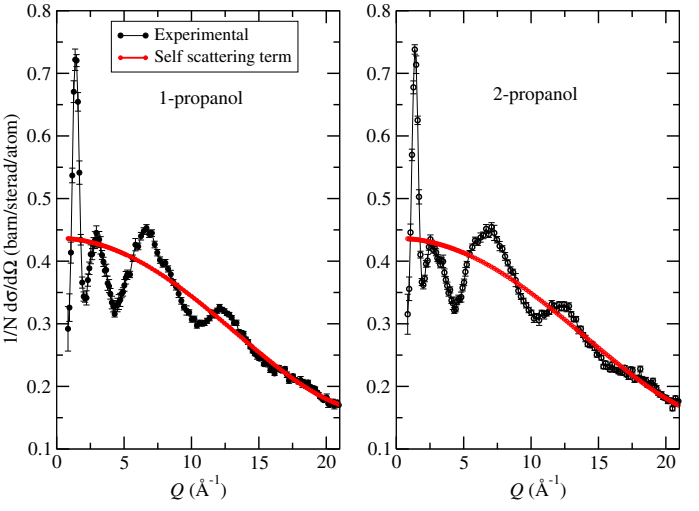

Figure 4. (colour online) Normalized coherent differential cross sections for 1-propanol and 2-propanol. The solid lines show the corresponding self scattering term ($P(Q)$ in Equation (4)).

cross sections and scattering lengths are taken from the recent compilation by Dawidowski et al. [28].

We stop the iterative process when the difference in the correction factors from two successive iterations is less than 0.5%. For both molecules, the convergence was achieved after three iterations (each run consisting in 200,000 neutron histories). The converged correction factors are then used to correct the experimental intensities and obtain the microscopic sought differential cross sections (see [13, Equation (1)]).

5. Results

Figure 3 shows the NSF and SF experimental intensities for 1-propanol and their different scattering components as obtained in the last iteration (single, multiple and total scattering). Besides the good agreement between the experimental data and the simulations, we observe that most of the measured signal is due to the single scattering ($\sim 94\,\%$), as expected for the annular sample geometry and the long mean free path for deuterated molecules.

Performing a simple linear combination of the corrected NSF and SF (Equation 2) intensities, we extract the corrected experimental coherent intensity $I^{\mathrm{coh}}_{\mathrm{corr}}(Q)$ [13]:

$$I^{\mathrm{coh}}_{\mathrm{corr}}(Q) = I^{\mathrm{S}}_{\mathrm{corr}}(Q)^{\mathrm{NSF}} - \frac{1}{2}\, I^{\mathrm{S}}_{\mathrm{corr}}(Q)^{\mathrm{SF}}. \tag{3}$$

The diffractogram from the vanadium rod is treated in a similar fashion, using a free gas model as energy transfer kernel and then used to normalize the propanol results. The resulting coherent differential cross section ($\frac{1}{\mathrm{N}}\frac{\mathrm{d}\sigma}{\mathrm{d}\Omega}$), in absolute units, is related to the static structure factor $S(Q)$:

$$\frac{1}{\mathrm{N}}\frac{\mathrm{d}\sigma}{\mathrm{d}\Omega} = \overbrace{\frac{\bar{\sigma}_{\mathrm{c}}}{4\pi}\left[S(Q)-1\right]}^{\text{interference}-\text{scattering term}} + \overbrace{\left[a_0 + a_2 Q^2 + a_4 Q^4\right]}^{\text{self}-\text{scattering term} = P(Q)}, \tag{4}$$

where $\bar{\sigma}_c$ is the average coherent cross section of the molecule and a_i are the coefficients in the Placzek's polynomial correcting for inelastic effects [29]. Figure 4 shows the normalized coherent differential cross section and the $P(Q)$ polynomial (self-scattering term) for 1- and 2-propanol. At high-Q, we observe the characteristic "fall-off" feature due to the interaction of the incident neutrons with the vibrating scattering sites [30]. By fitting $\frac{1}{N}\frac{d\sigma}{d\Omega}$ with $P(Q)$ in the high-Q region ($Q \geq 5\,\text{Å}^{-1}$), we obtain the coefficients a_i as: $a_0 = 0.437(6)$, $a_1 = -1.02(6) \times 10^{-3}$, $a_2 = 0.95(13) \times 10^{-6}$ for 1-propanol and $a_0 = 0.438(6)$, $a_1 = -0.96(6) \times 10^{-3}$, $a_2 = 0.79(10) \times 10^{-6}$ for 2-propanol. We note that the a_0 values, limit of $P(Q)$ at $Q = 0$, are consistent with the expected value, which is the average coherent bound cross section, $P(0) = \frac{\bar{\sigma}_c}{4\pi} = 0.4354(5)$ barn/steradian/atom [28]. Then, subtracting $P(Q)$ from $\frac{1}{N}\frac{d\sigma}{d\Omega}$ and performing simple algebraic operations, we obtain the static structure factors, as shown in Figure 5.

6. Discussion

Equations (1) and (2) are similar to the equivalent ones commonly employed in correcting data for liquid and amorphous materials, but important conceptual differences here require a deeper discussion.

The standard methods [2–4] consider the attenuation and multiple scattering as independent corrections applied successively, usually performing the attenuation correction first and then the multiple scattering ones. The attenuation factors are calculated using the expressions derived by Paalman and Pings [31], which are only valid for single and elastic scattering. The multiple scattering corrections are usually performed using the expressions of Blech and Averbach [32]. These are derived assuming elastic and isotropic scattering and lead to a constant contribution, in contrast with our non-constant multiple scattering contribution (Figure 3).

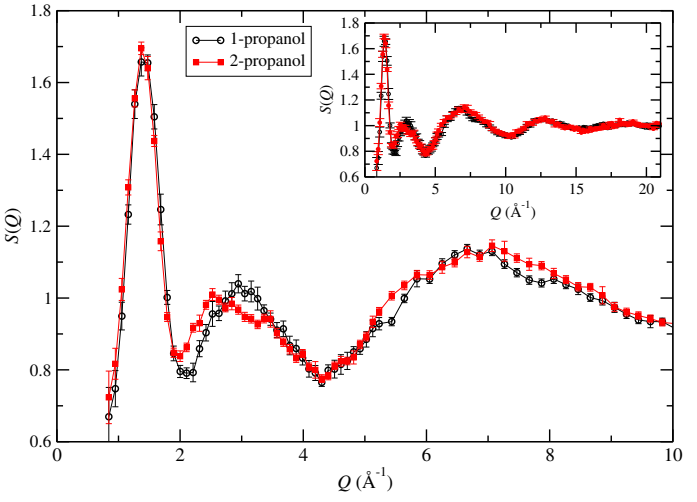

Figure 5. (colour online) Normalized static structure factor for 1- and 2-propanol (open and full symbols, respectively) in the low- and medium-Q regions. The inset shows the whole Q-range.

The main advantage of our MC procedure is that we treat the problems of attenuation, multiple scattering, inelasticity and anisotropy as a whole. For the attenuation correction, we also take into account the energy exchange after each interaction (non negligible for light atoms), not only for singly scattered neutrons but also for those scattered several times in the sample and/or in the container. For both corrections, we take into account the anisotropy of the scattering law, generally neglected by the traditional methods. As we follow the whole history of each neutron in the MC simulation, we are able to consider all these effects in a consistent manner. As an example, in Figure 3, we show the multiple scattering contribution to the NSF and SF diffractograms and the merged multiple scattering + attenuation correction factors from Equation (2). Both show a clear Q-dependence resembling that of the experimental curve, something that traditional methods do not reflect.

However, while the present model is useful for coherent samples, it still needs some improvement when the incoherence increases. The main difficulty is found in Equation (32) of Ref. [26], which represents the contribution of a neutron history to the detected signal. In the case of coherent samples, we have proved that the double differential cross section can be separated into an angular distribution and a narrow energy transfer kernel (see [26, Equation (34)]). Particularly, in the case of deuterated propanol, the differences using Equations (32) or (34) [26] are less than 0.5%. This assumption represents an important simplification of the contribution to the signal and considerably reduces the computing time. Such an approximation is no more valid for incoherent samples, for which the complete evaluation of Equation (32) [26] is necessary. This improvement of our correction method is still under development.

As for the structure factors, a careful observation of Figure 5 gives some insight into the intra- and inter-molecular structures. We can distinguish three different regions: a high-Q region above 10 Å^{-1}, a low-Q region below 2 Å^{-1} and a medium-Q region in between. The high-Q region corresponds to very short distances in real space (less than 0.7 Å), where we do not expect any difference in the molecular structure. The similarity of both structure factors is then fully justified. The low-Q region has only the main peak, which corresponds to the size of the molecules. For 1- and 2-propanol, the peaks appear at 1.43 and 1.40 Å^{-1}, corresponding to 4.38 and 4.49 Å, which are more or less the dimensions of the molecules. The FWHM of this peak for both molecules is about 0.5 Å^{-1} indicating that the inter-molecular correlation is lost after 12.5 Å, i.e. about 3 molecular sizes. In the medium-Q range, we expect a mixture of intra- and inter-molecular correlations. The main feature is the double peak observed for 2-propanol. The peak at 2.58 Å^{-1} could correspond to the distance between the O and a D in a methyl group, a correlation that should be more important for 2-propanol than 1-propanol. Also in this region, we observe a peak at 3.05 Å^{-1} for 1-propanol, which could correspond to the correlation between the D in the hydroxyl group and the D bonded to the nearest C atom.

In the case of 2-propanol, in Figure 6 we compare our static structure factor with those obtained by Sahoo et al. (reactor experiment) [11] and Zetterström et al. (time-of-flight experiment) [33], focusing our analysis on the low-Q region, around and below 2 Å^{-1}. We obtain a main peak position and width very close to those from Sahoo et al., and discrepancies below 1 Å^{-1} and beyond 2.5 Å^{-1} could originate from an improper background subtraction linked to the standard correction method, which neglects the inelasticity effects in the attenuation factors. On the other hand, our results show a good agreement with the Zetterström et al. data above 1 Å^{-1}, except for the width of the main peak. This is likely related to the different resolution functions in reactor and spallation experiments.

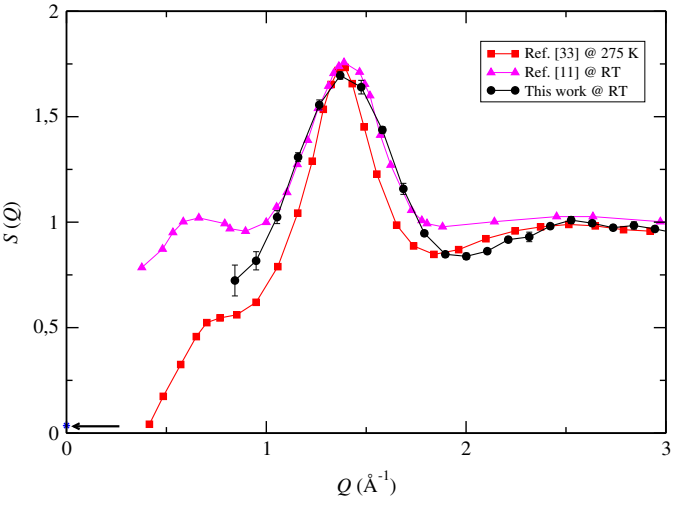

Figure 6. (colour online) Comparison of our static structure factor for 2-propanol at low-Q with that from the literature (Sahoo et al. [11] and Zetterström et al. [33]). The horizontal arrow points to the $S(0)$ ($= k_{\mathrm{B}}T\ \rho\ \chi_T$).

Below 1 $\mathrm{Å}^{-1}$, the three sets of data give different results. However, all data should tend to the thermodynamic limit $S(0) = k_{\mathrm{B}}T\ \rho\ \chi_T$ [27], where k_{B} is the Boltzmann's constant and T is the temperature. For 2-propanol, this value is 0.0358 (see horizontal arrow in Figure 6). The Sahoo et al. data [11] show a rather high contribution at low-Q, which seems incompatible with the limiting value of the structure factor. On the other hand, Zetterström et al. [33] present a strange behaviour with a slope that can hardly be consistent with a positive value of χ_T. Due to experimental constraints, we were not able to observe the pre-peak at 0.8 $\mathrm{Å}^{-1}$ but, taking into account the trends of three sets, we could infer that our data are in the best position to be compatible with the limiting value at $Q = 0$.

7. Conclusions

We have presented a procedure to correct the NSF/SF diffractograms obtained from polarized neutron diffraction experiments with polarization analysis. This improved methodology for determining the experimental scattering intensities produced by the sample alone ($I^{\mathrm{S}}(Q)^{\mathrm{NSF,SF}}$), leads to a more precise differential scattering cross section than the traditional methods.

In the evaluation of the neutron total cross section and the energy-transfer kernel for propanol, it was necessary to construct a synthetic model, providing the input parameters. For 1-propanol this task was relatively easy, thanks to the similarity of this molecule with ethanol, for which these parameters were already determined [25]. For the 2-propanol molecule, we had to recalculate the effective masses for the CD unit, not present in ethanol. Our MC code allowed us to determine the static structure factors for 1- and 2-propanol, performing all the corrections (background, container, attenuation, multiple scattering and inelasticity) in a consistent way. We also showed that some assumptions, such as a

Q-independent multiple scattering contribution, made in the traditional methods, are not valid (see Figure 3).

It is worth noting that a Placzek correction is still necessary, because the isotopic incoherence and the inelastic coherent scattering cannot be experimentally removed. The main improvement of this method is its ability to actually measure a big fraction of the incoherent scattering, making the Placzek correction smaller and hence resulting in more accurate structure factors.

The results obtained for 2-propanol were compared with those obtained by Sahoo et al. [11] and Zetterström et al. [33], showing that our methodology produces consistent and coherent results, even if there are some small discrepancies that could be ascribed to the different methodologies. We showed the need of completing the measurement at low-Q to settle the question of which of the three data-sets is the most plausible.

We have only presented results for deuterated samples, as the correction method has yet to be extended to the case of highly incoherent samples. However, we argue that the proposed method will allow the determination of the static structure factor also for protonated (normal) samples. Already, at the experimental level, it allows a separation of the coherent and incoherent contributions to the total scattering, drastically reducing the background in the coherent part. The obtained intensities can then be corrected afterwards, either by traditional [2–4] or new [1,13] methods.

Finally, we hope that this work will help improving the tools used in processing, analysing and correcting the experimental data from neutron diffraction experiments with (and without) polarization analysis. The algorithm developed here is intended for the benefit of the neutron diffraction user community, even if we must admit that a model of interaction between the neutron and the nuclei is necessary. We showed that for simple molecular systems like alcohols, propanol in our case, the Synthetic Model is well adapted for this purpose.

Acknowledgements

The authors thank Sebastien Vial for the technical support during the experiments on D3. The beam time provided by the Institut Laue Langevin (Grenoble, France) is gratefully acknowledged (proposal 6-02-543) [12]. JD and LARP wish to thank Argentinean Council for Scientific and Technological Research (CONICET) and Argentinean Agency for Scientific and Technological Promotion (ANPCyT) for the financial support via the [grant number PIP-11220110100552], [PICT-2011-534], respectively.

Disclosure statement

No potential conflict of interest was reported by the authors.

Funding

This work was supported by Argentinean Council for Scientific and Technological Research (CONICET) [grant number PIP-11220110100552]; Argentinean Agency for Scientific and Technological Promotion (ANPCyT) for the [grant number PICT-2011-534].

References

[1] L. Temleitner, A. Stunault, G.J. Cuello and L. Pusztai, Phys. Rev. B 92 (2015) p.014201.
[2] M.A. Howe, R.L. McGreevy and P. Zetterström, Computer Code CORRECT, NFL Studsvik, 1996.
[3] G.J. Cuello, J. Phys.: Cond. Matter 20 (2008) p.244109.
[4] H.E. Fischer, A.C. Barnes and P.S. Salmon, Rep. Prog. Phys. 69 (2006) p.233.
[5] C.J. Benmore and Y.L. Loh, J. Chem. Phys. 112 (2000) p.5877.
[6] T. Yamaguchi, C.J. Benmore and A.K. Soper, J. Chem. Phys. 112 (2000) p.8976.
[7] Y. Tanaka, N. Ohtomo and K. Arakawa, Bull. Chem. Soc. Japan 58 (1985) p.270.
[8] G.J. Cuello, C. Talón, C. Cabrillo and F.J. Bermejo, Appl. Phys. A: Mat. Sci. Process. 74 (2002) p.S552.
[9] C. Talón, F.J. Bermejo, C. Cabrillo, G.J. Cuello, M.A. González, J.W. Richardson Jr, A. Criado, M.A. Ramos, S. Veira, F.L. Cumbrera and L.M. González, Phys. Rev. Lett. 88 (2002) p.115506.
[10] A. Sahoo, S. Sarkar, P.S.R. Krishna, V. Bhagat and R.N. Joarder, PRAMANA-J. Phys. 71 (2008) p.133.
[11] A. Sahoo, S. Sarkar, P.S.R. Krishna and R.N. Joarder, PRAMANA-J. Phys. 74 (2010) p.765.
[12] G.J. Cuello, J. Dawidowski, L.A. Rodríguez Palomino, and A. Stunault, Institut Laue–Langevin. (2014), doi:10.5291/ILL-DATA.6-02-543.
[13] L.A. Rodríguez Palomino, A. Stunault, J. Dawidowski, L. Temleitner, L. Pusztai and G.J. Cuello, J. Phys.: Conf. Series. (2015, in press).
[14] A. Stunault, S. Vial, L. Temleitner, G.J. Cuello and L. Pusztai, J. Phys.: Conf. Series. 2015 in press.
[15] J. Dreyer, L.P. Regnault, E. Bourgeat-Lami, E. Lelièvre-Berna, S. Pujol, F. Thomas, M. Thomas and F. Tasset, Nucl. Instr. Meth. Phys. Res. A 449 (2000) p.638.
[16] W. Heil, J. Dreyer, D. Hofmann, H. Humblot, E. Lelièvre-Berna and F. Tasset, Physica. B 267–268 (1999) p.328.
[17] Sigma-Aldrich Co, Available at http://www.sigmaaldrich.com
[18] V.F. Sears, Adv. Phys. 24 (1975) p.1.
[19] F.G. Bischoff, *Generalizad Monte Carlo method for multiple scattering problems in neutron and reactor physics*, Ph.D. thesis, Rensselaer Polytechnic Institute, 1969.
[20] J.R.D. Copley, P. Verkerk, A.A. van Well and H. Fredrikze, Comput. Phys. Comm. 40 (1986) p.337.
[21] C. Rodrigues, A. Vinhas, S.B. Herdade and L.Q. Do, Amaral: J. Nucl. Energy 26 (1972) p.379.
[22] J.R. Granada, Phys. Rev. B 31 (1985) p.4167.
[23] J.R. Granada, Phys. Rev. B 32 (1985) p.7555.
[24] J.R. Granada, J. Dawidowski, R.E. Mayer and V.H. Gillette, Nucl. Instr. Meth. Phys. Res. A 261 (1987) p.573.
[25] J. Dawidowski, J.R. Granada and J.J. Blostein, Nucl. Instr. Meth. Phys. Res. B 168 (2000) p.462.
[26] L.A. Rodríguez Palomino, J. Dawidowski, J.J. Blostein and G.J. Cuello, Nucl. Instr. Meth. Phys. Res. B. 258 (2007), p. 453.
[27] G.L. Squires, *Introduction to the Theory of Thermal Neutron Scattering*, Dover Publications Inc, Mineola, New York, NY, 1978. ISBN 0-486-69447-X.
[28] J. Dawidowski, J.R. Granada, J.R. Santisteban, F. Cantargi and L.A. Rodríguez Palomino, *Experimental methods in physical sciences*, in *Neutron Scattering Fundamentals*, F. Fernández-Alonso and D.L. Price, eds. Elsevier Inc, Oxford, 2013, p. 471.
[29] G. Placzek, Phys. Rev. 86 (1952) p.377.
[30] P.P. Nath, S. Sarkar, P.S.R. Krishna and R.N. Joarder, Z. Naturforsch A 56 (2001) p.825.
[31] H.H. Paalman and C.J. Pings, J. Appl. Phys. 33 (1962) p.2635.
[32] I.A. Blech and B.L. Averbach, Phys. Rev. 137 (1965) p.A1113.
[33] P. Zetterström, U. Dahlborg, R.G. Delaplane and W.S. Howells, Phys. Scr. 44 (1991) p.56.